AIAA JOURNAL
Vol. 37, No. 11, November 1999

Effect of Isolated Micron-Sized Roughness on Transition in Swept-Wing Flows

Ronald H. Radeztsky Jr.,* Mark S. Reibert,† and William S. Saric‡
Arizona State University, Tempe, Arizona 85287-6106

Boundary-layer transition-to-turbulence studies are conducted in the Arizona State University Unsteady Wind Tunnel on a 45-deg swept airfoil. The pressure gradient is designed so that the initial stability characteristics are purely crossflow dominated. Flow-visualization and hot-wire measurements show that the development of the crossflow vortices is influenced by roughness near the attachment line. Comparisons of transition location are made between a painted surface (distributed 9-μm peaks and valleys on the surface), a machine-polished surface (0.5-μm rms finish), and a hand-polished surface (0.25-μm rms finish). Then isolated 6-μm roughness elements are placed near the attachment line on the airfoil surface under conditions of the final polish (0.25-μm rms). These elements create an enhanced packet of stationary crossflow waves, which results in localized early transition. The diameter, height, and location of these roughness elements are varied in a systematic manner. Spanwise hot-wire measurements are taken behind the roughness element to document the enhanced vortices. These scans are made at several different chord locations to examine vortex growth.

Nomenclature

c	= chord
D	= diameter of roughness
k	= height of roughness
N	= linear stability amplification factor, $\ell_n(u'/u'_0)$
Re_c	= chord Reynolds number
Re_k	= roughness Reynolds number
x	= distance along chord, m
x_{tr}/c	= transition location
y	= wall-normal coordinate, m
z	= distance along span, m
α	= angle of attack
λ	= stationary crossflow vortex wavelength along span
λ_{cf}	= stationary crossflow vortex wavelength
ω	= traveling-wave frequency

I. Introduction

THE present investigation is a continuation of previous efforts to determine the fundamental nature of the crossflow instability that is characteristic of the breakdown to turbulence in three-dimensional boundary layers that are found in swept-wing flows. Reviews of the current literature and problems are given by Reed and Saric[1] and Reed et al.[2]

This experiment uses the NLF(2)-0415 airfoil[3] as the basic test configuration. The model has a pressure minimum on the upper surface at approximately $x/c = 0.71$ (see Fig. 1) and, thus, is an ideal crossflow generator when swept. Specially designed wall liners within the wind-tunnel nozzle and test section produce an infinite swept-wing flow with no spanwise gradients.[4] Standard boundary-layer codes[5] are used for this configuration. The pressure fields and undisturbed boundary-layer profiles have been thoroughly documented and are in agreement with the calculations.[4,6]

With a 45-deg sweep and a small negative angle of attack, the favorable pressure gradient produces a boundary-layer flow that is subcritical to Tollmien–Schlichting (T–S) wave formation at moderate chord Reynolds numbers, but produces considerable crossflow. This permits the isolated examination of the crossflow stability problem. The instability at $\alpha = -4$ deg was analyzed using the MARIA and SALLY stability codes. Although it is recognized that more complete codes can be used, e.g., by Reed et al.,[2] these were used primarily as design codes to produce a general picture of the stability behavior. At a chord Reynolds number of $Re_c = 3.8 \times 10^6$, the maximum predicted N factor is $N = 16.0$ for $f = 200$ Hz. Dagenhart[7] indicates that, according to standard N-factor correlation methods, transition may be expected for N factors in the range from 9 to 11. Thus, for sufficiently high Reynolds numbers (less than 3.8×10^6), the transition due to crossflow vortex amplification is expected to occur well ahead of the pressure minimum at $x/c = 0.71$. The fundamental linear stability results for this configuration are complete and include the wavelengths, local growth rates, frequencies, and evolution patterns of the crossflow vortices in the linear range.[8–10] In this work, the frequencies of the crossflow instability are observed to establish the existence of the theoretically predicted moving crossflow vortices in addition to stationary crossflow vortices.

Whereas linear stability theory predicts that the traveling crossflow waves are more amplified than the stationary crossflow waves, many experiments observe stationary waves. The answer to the question of whether one observes stationary or traveling crossflow waves is cast inside the receptivity problem. One of the key missing ingredients in many three-dimensional boundary-layer experiments is the understanding of receptivity and initial conditions. Here, receptivity refers to the mechanisms that cause environmental disturbances to enter the boundary layer and cause unstable waves.[11] Receptivity has many different paths through which to introduce a disturbance into the boundary layer. They include the interaction of freestream turbulence and sound with model vibrations, leading-edge curvature, discontinuities in surface curvature, or surface roughness. Any one or a combination of these may lead to unstable waves in the boundary layer. If the initial amplitudes of the disturbances are small, they will tend to excite the linear normal modes of the boundary layer.

The importance of environmental conditions in the crossflow problem is illustrated by comparing equivalent experiments in different facilities. Bippes and Müller[12] and Bippes[13] describe a series of comparative experiments in a low-disturbance tunnel and a high-disturbance tunnel. Their results show that traveling crossflow waves are observed in the high-disturbance tunnel rich in unsteady freestream disturbances and that the dominant boundary-layer structure in a low-disturbance tunnel is a stationary crossflow vortex. Because the flight environment is more benign than the wind tunnel,

Presented as Paper 93-0076 at the AIAA 31st Aerospace Sciences Meeting, Reno, NV, 11–14 January 1993; received 21 September 1996; revision received 1 August 1998; accepted for publication 28 March 1999.

*Assistant Research Professor, Mechanical and Aerospace Engineering. Member AIAA.

†Faculty Research Associate; currently Senior Software Engineer, Datasoft Corp., 7669 Myrtle Avenue, Tempe, AZ 85284. Member AIAA.

‡Professor, Mechanical and Aerospace Engineering. Associate Fellow AIAA.

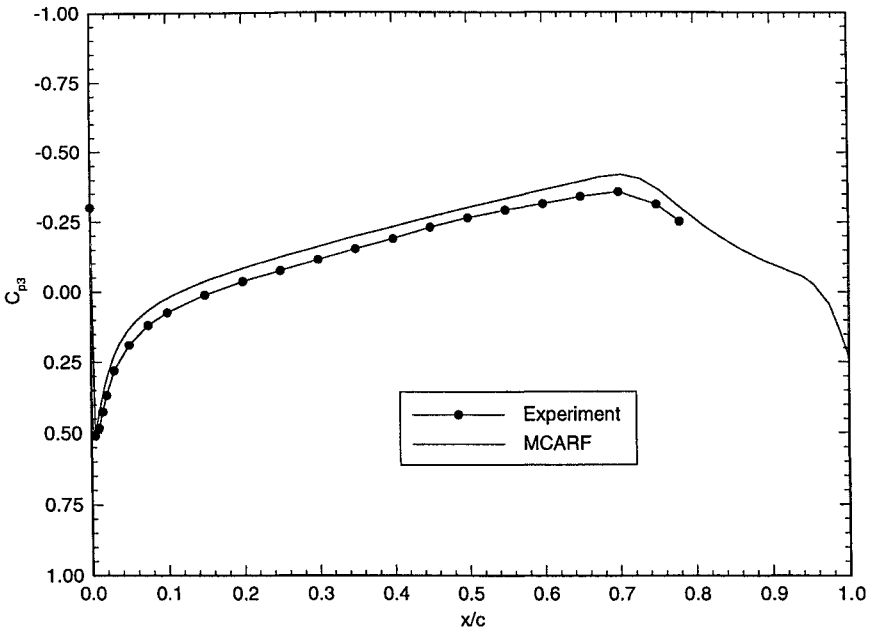

Fig. 1 NLF(2)-0415 upper-surface pressure distribution in wind tunnel at $\alpha = -4$ deg.

one expects the low-disturbance results to be more important. Recent work by Deyhle et al.[14] and Deyhle and Bippes[15] confirms these earlier results. However, there was no attempt to separate sound levels from turbulence levels within the freestream disturbance environment. In Sec. II.C, we conclude that the Bippes and Müller[12] effect is due to turbulence.

The nonlinear processes that control transition are documented by Kohama et al.[16] In this work, the stationary crossflow vortex is shown to be the harbinger of transition by causing a high-frequency secondary instability that results from distortions in the steady boundary-layer flow. Thus, crossflow transition in a low-disturbance environment is determined by the characteristics of the stationary wave.

The receptivity problem for stationary waves is dominated by small-scale surface roughness rather than turbulence. This is suggested by Dagenhart,[4] who observed that transition patterns due to stationary crossflow waves on the NLF(2)-0415 airfoil remained fixed throughout many test entries, even with changes in the turbulence-treatment section of the wind tunnel. This is also consistent with the observation of Bippes and Müller[12] that the stationary crossflow transition pattern remains fixed relative to their flat-plate model when the model is translated laterally in the test section. Thus, the present work concentrates on the role of surface roughness in influencing swept-wing transition.

II. Results

A. Distributed Micron-Sized Roughness Due to Surface Finish

The transition measurements in this part of the study are obtained from naphthalene flow visualization. This technique relies on the sublimation patterns of the naphthalene to identify the stationary crossflow structure and the location of transition. The naphthalene technique was calibrated in previous experiments by the use of surface-mounted hot films, hot wires, and liquid crystals[4,9,17] and has been shown to provide very reliable measurements of transition for the stationary patterns studied here. Surface roughness measurements were done by taking castings of the surface with a dental pattern resin that created a rigid sample suitable for profilometer measurements. The accuracy of the casting method was calibrated by making castings of submicrometer reference grooves on a steel block. Although the casting method is locally accurate to better than 0.1 μm, the larger scales, including those of interest for crossflow, are dominated by warping of the sample. Thus, the distributed roughness amplitudes presented here serve to compare the character of various model surfaces, but the samples are not suitable for spectral analysis at the crossflow wavelengths.

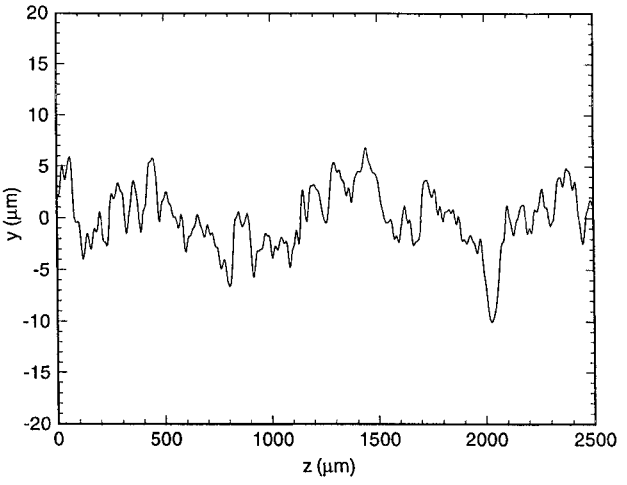

Fig. 2 Profilometer measurement of NLF(2)-0415 surface roughness: painted surface, filtered 20–1500 μm, rms = 3.30 μm.

Figure 2 shows the surface characteristics of the original painted model. This surface was used for all of the previous experiments.[4,8–10,16] The peak-to-peak roughness in this case is around 8–10 μm. For the present experiment, the paint was removed, and the surface was sanded and machine polished to the level of Fig. 3. Here the surface finish is 0.5 μm rms. The model was then subjected to a systematic hand polish, and the surface finish was reduced to 0.1 μm rms in the midchord region and 0.25 μm rms near the attachment line as shown in Fig. 4.

Transition measurements were conducted at a number of different chord Reynolds numbers Re_c, under the conditions of the different surface finishes just described. With random distributed surface roughness, the transition front is a fixed, jagged pattern of merging turbulent wedges beginning in areas where the stationary crossflow waves have produced strongly inflected mean profiles as described by Kohama et al.[16] The earliest transition wedges, i.e., those beginning at the lowest x/c, are correlated in the spanwise position with distinct imperfections in the paint finish near the attachment line. Thus, the initiation of transition due to stationary crossflow is a local event and is not described by a single x/c for the entire model, even though the transition location at any particular spanwise location is very well defined and repeatable. Following Dagenhart,[4] the average transition location x_{tr}/c is defined as the spanwise average of

Table 1 Transition location as a function of roughness height[a]

k, μm	x_{tr}/c	$N(\omega=0)$[b]	N[c]	Re_k
9.0	0.40	5.5	7.1	0.30
0.5	0.61	8.4	11.0	$<10^{-3}$
0.25	0.68	9.2	11.8	$<10^{-3}$

[a] $Re_c = 2.7 \times 10^6$.
[b] Amplification factor for the most amplified stationary crossflow wave.
[c] Amplification factor for the most amplified traveling wave.

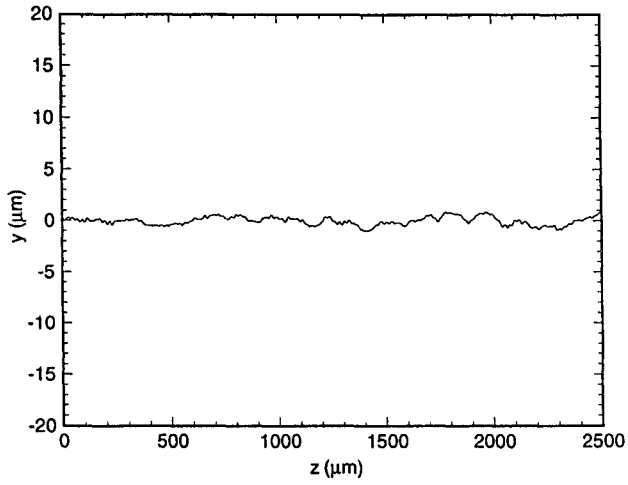

Fig. 3 Profilometer measurement of NLF(2)-0415 surface roughness: first polish, filtered 20–1500 μm, rms = 0.509 μm.

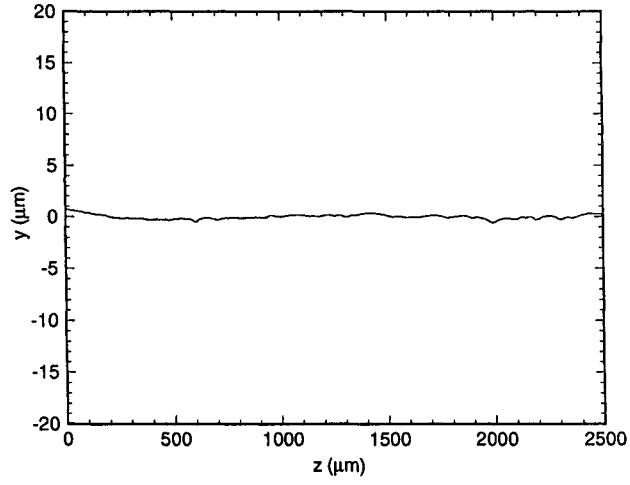

Fig. 4 Profilometer measurement of NLF(2)-0415 surface roughness: hand polish, filtered 20–1500 μm, rms = 0.121 μm.

the observed transition front revealed by the naphthalene. In Fig. 5, x_{tr}/c is shown to increase with subsequent levels of polishing of the model. The painted-surface results are from Dagenhart et al.[9] The polished-surface results show quite dramatically the effect of surface finish and the sensitivity to even small changes in surface roughness. Table 1 is an example from one typical chord Reynolds number.

B. Isolated Roughness Elements

Using the hand-polished surface as a clean base configuration, isolated roughness elements are applied near the attachment line to clearly reveal the effect of surface roughness on transition due to stationary crossflow waves. The roughness elements are obtained by applying rub-on symbols from transfer sheets commonly used in the graphic arts. The dimensions of the applied elements are calibrated by repeatedly applying them to an aluminum block. The applied

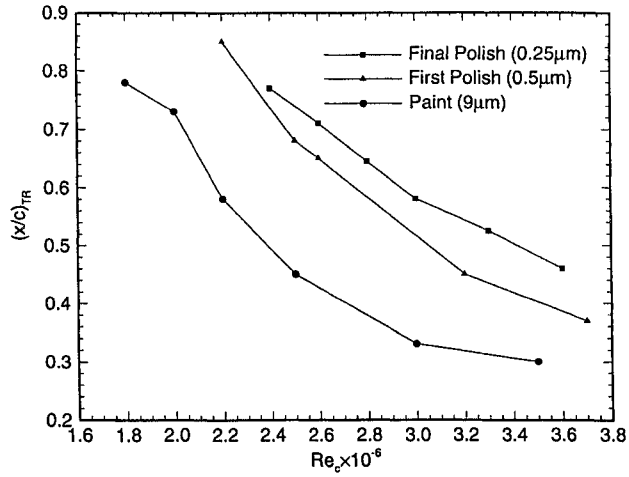

Fig. 5 Naphthalene visualization results showing average transition location vs chord Reynolds number for three different surface finishes; paint roughness is measured peak-to-peak; polished roughness is rms.

elements are carefully measured using a dial-indicator displacement gauge and a profilometer. The average height of the elements is 6 μm. The surface of the elements is uneven, with thickness variations of approximately 20%. Taller elements are created by stacking the 6-μm dots. Careful measurements indicate a mean thickness of 6 μm per layer, with very little compression of the lower layers. The sides of the elements are not perfectly straight because the pressure applied during installation spreads the material slightly at the edges.

The roughness Reynolds number Re_k value for these roughness elements ranges from 0.12 to 4.5 and is well below the threshold for the direct-tripping transition mechanism studied by von Doenhoff and Braslow.[18] The direct-tripping mechanism for three-dimensional roughness is operative at high roughness Reynolds number values ($\gg$100), and is due to a wake instability in the flow directly behind the roughness element. (von Doenhoff and Braslow refer to this as a T–S instability, but it is neither T–S nor crossflow.) As such, it is basic-state independent, and any influence on the linear stability part of the process is bypassed. The recent experiments of Juillen and Arnal[19] confirm the von Doenhoff and Braslow[18] correlation for large roughness in three-dimensional boundary layers. In contrast, the present results show how very small roughness influences the initial conditions for the linear stability part of crossflow-vortex amplification.

When an isolated 6-μm roughness element (3.7-mm diam) is introduced at $x/c = 0.023$, a single distinct turbulent wedge appears against the mostly laminar background, with a vertex positioned at $x_{tr}/c = 0.40$. The position of the vertex provides a well-defined measure of transtion location due to the isolated roughness (in contrast with the distributed-roughness case) and is repeatable to within $0.01c$. Hot-wire measurements confirm the beginning of transition at this point.

The naphthalene flow visualization reveals that the early transition occurs in the vicinity of the particular stationary crossflow vortex that passes near the roughness location, and the signature of the stationary crossflow vortices in the naphthalene along the path from the roughness to the transition vertex is stronger than the background. This observation is quantified with hot-wire measurements (as described later) and clearly shows that the effect of the roughness is to provide higher local initial amplitudes for the stationary crossflow waves, which lead to transition at a lower N factor than in the clean-surface case.

1. *Roughness Location*

The effect of roughness location is determined by systematically applying single 6-μm elements at chord locations between $x/c = 0.005$ and $x/c = 0.045$. Figure 6 clearly shows that the transition location is very sensitive to the roughness position. For the data shown, the attachment line is at $x/c = 0.007$, and the calculated neutral stability point for the most unstable stationary modes is at $x/c = 0.02$. The x_{tr}/c location may be computed by using the chord

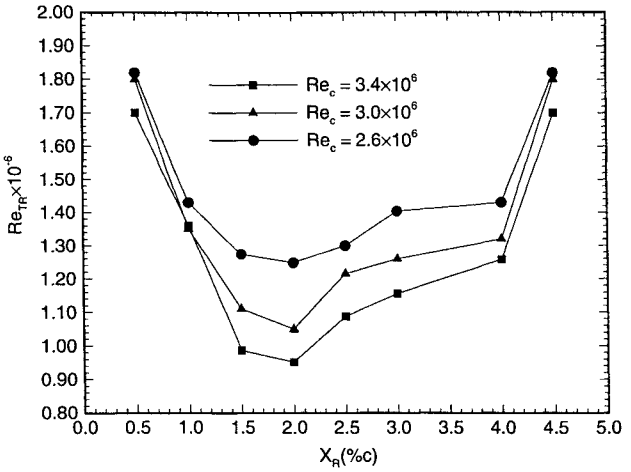

Fig. 6 Variation of transition Reynolds number with roughness x/c at three chord Reynolds numbers; single roughness element is used with $D = 3.7$ mm, $k = 6$ μm.

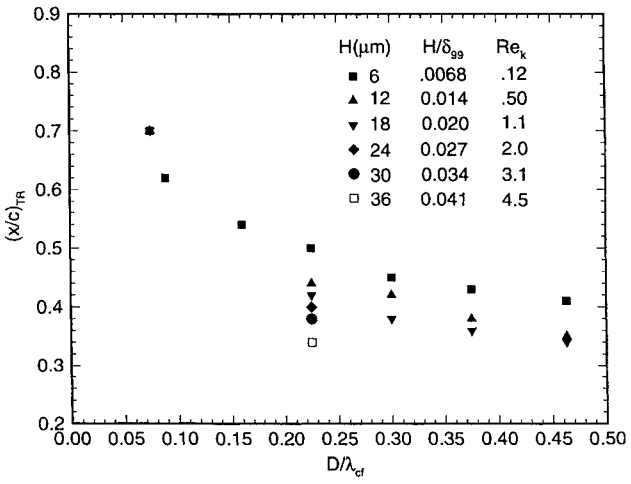

Fig. 7 Transition location as a function of roughness height and diameter; single roughness element is at $x/c = 0.023$; $Re_c = 2.6 \times 10^6$.

Reynolds number values given in Fig. 6. When the roughness is located upstream of the neutral stability point, the crossflow modes influenced by the roughness will initially decay, so that the influence of the roughness is minimized. For roughness too far downstream of the neutral point, the influence is also minimized, with roughness beyond $x/c = 0.04$ having no effect on the transition location at least for $Re_k < 4.5$. When the roughness is located outside of the narrow band around the neutral stability point, the transition Reynolds number returns to the no-roughness value. This result justifies a posteriori the use of naphthalene in the midchord region.

2. Roughness Size

To more fully characterize the effect of isolated roughness near the attachment line, a variety of roughness sizes were introduced at $x/c = 0.023$. Roughness diameters D ranged from 0.3 to 3.7 mm, which corresponds to 0.08 to 0.5 times the dominant stationary crossflow vortex wavelength λ_{cf}. Heights varied between 6 and 36 μm. The roughness Reynolds number Re_k based on roughness height and local velocity ranged from 0.12 to 4.5. Flow-visualization measurements reveal a strong dependence of transition-wedge location on both the roughness height and the roughness diameter, as shown in Fig. 7. The transition location moves forward for the larger diameters and heights and moves downstream as the roughness height or diameter is reduced. Figure 7 also shows that for the smallest roughness diameter tested, the transition wedge has retreated to the $x/c = 0.71$ location and has merged into the natural background transition front associated with the clean baseline surface. Even if the roughness height is tripled to 18 μm, the transition

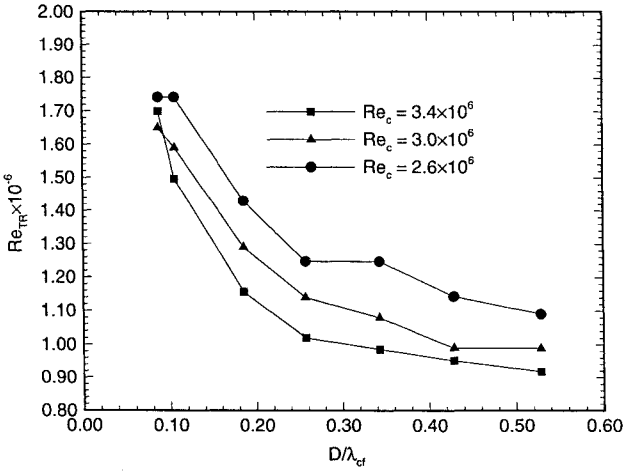

Fig. 8 Variation of transition Reynolds number with roughness diameter at three chord Reynolds numbers; roughness is located at $x/c = 0.023$.

wedge does not reappear, indicating that any effect of the small-diameter roughness on the stationary crossflow is very weak and has dropped below the background level of the experiment.

The effect of roughness diameter on transition is directly related to the Fourier spectrum of the roughness element and its relation to the dominant stationary crossflow wavelengths. Although the analysis is more complicated for the continuous spectrum of an isolated three-dimensional element than for the discrete spectrum of a uniform spanwise roughness distribution, the result is similar. As the roughness diameter decreases, the coupling between the roughness spectrum and the dominant crossflow modes decreases rapidly. This effect was investigated by Choudhari,[20] who obtained results that are consistent with the present observations.

The effect of roughness diameter on the transition location was studied at three different unit Reynolds numbers. The results are shown in Fig. 8, which shows transition Reynolds number vs roughness diameter. The x_{tr}/c location may be obtained by scaling transition Reynolds number by chord Reynolds number. Again, as the roughness diameter becomes small, the transition location returns to the no-roughness location because the effect of the roughness drops below the background. In Fig. 8, it is clear that the dependence of transition on chord Reynolds number is not really a unit Reynolds number effect but instead is a roughness Reynolds number effect.

These measurements illustrate the importance of both the roughness height, as measured by roughness Reynolds number, and of spanwise scale, vis à vis with λ_{cf}, in assessing the role of surface roughness. Note that these conclusions are for $Re_k < 4.5$. Obviously, very large roughness heights, even with small diameters (like paint specks), could cause early transition through the direct-tripping mechanism discussed earlier.

3. Two-Dimensional Roughness

When a long (100 mm) spanwise strip of 6-μm roughness is applied at $x/c = 0.023$, early transition wedges appear downstream only on the stationary vortices that originate near the ends of the roughness strip. This shows that the roughness has a strong effect on the stationary crossflow only in those regions where the local spectrum of the roughness contains the appropriate scales. The wake behind the center regions of the strip is stable and has no measurable influence on the transition location.

C. Insensitivity to Freestream Sound

Sound, along with two- and three-dimensional roughness (following Saric et al.[21] for two-dimensional boundary layers), has no observable effects on transition. Sound pressure levels of up to 95 dB were introduced at all important frequencies, e.g., the frequency of the maximum amplified traveling crossflow wave, the frequency of a destabilized T–S wave, the frequency of the secondary instability, as well as broad-band sound, with negative results in each case. This further substantiates the important role of the stationary crossflow wave in causing transition in this flow condition.

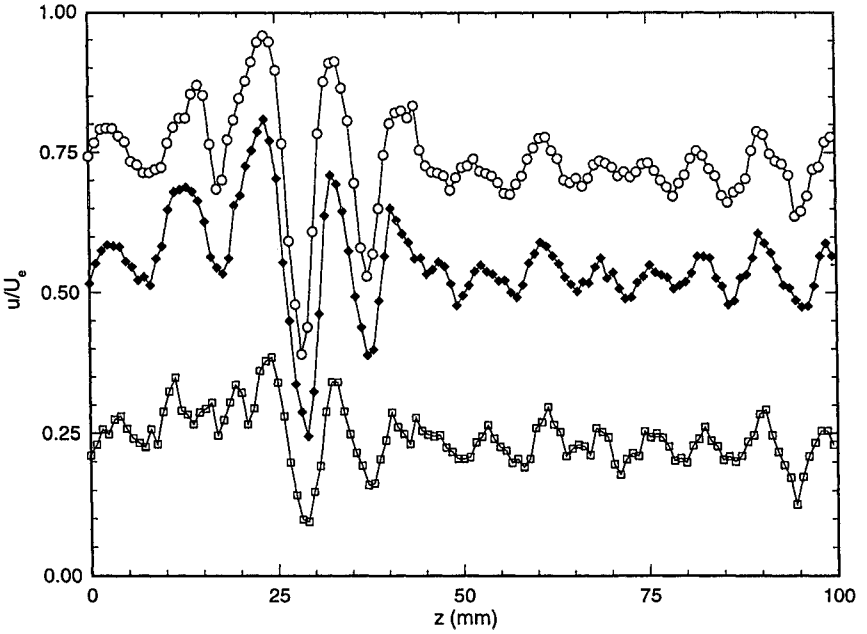

Fig. 9 Spanwise hot-wire scans at $x/c = 0.35$; constant-y scans at $\bar{u}/U_e = 0.25$, 0.50, and 0.75; single roughness element with $D = 3.7$ mm, $k = 6$ μm is at $x/c = 0.023$; $Re_c = 2.6 \times 10^6$.

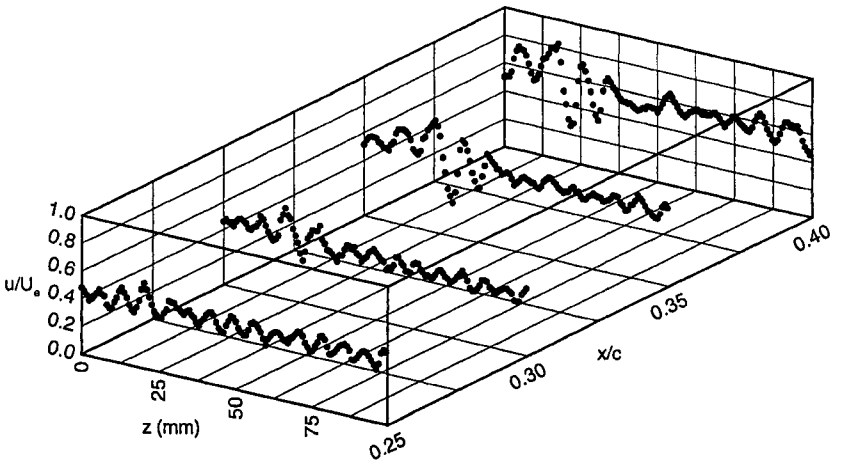

Fig. 10 Spanwise hot-wire scans showing streamwise vortex growth; constant-y scans at $\bar{u}/U_e = 0.50$; single roughness element with $D = 3.7$ mm, $k = 6$ μm is at $x/c = 0.023$; $Re_c = 2.6 \times 10^6$.

Moreover, it suggests that the Bippes and Müller[12] results are due to turbulence.

D. Hot-Wire Measurements

Detailed hot-wire measurements are made downstream of the isolated 6-μm roughness element to quantify further the behavior of the roughness-induced vortices. Because the stationary vortices are very weak, a direct measurement of the v' and w' velocities is impossible. However, when acting over large distances, these weak vortices produce strong distortions (10–50%) in the streamwise velocity profile, and this can be easily measured. The qualitative description of this follows Kohama et al.[16] In regions of $v' > 0$, low momentum fluid near the wall is entrained into the upper regions of the boundary layer. In regions of $v' < 0$, high momentum fluid is driven downward. Thus, very small v' can produce $\mathcal{O}(1)$ changes in the mean streamwise velocity. This behavior is responsible for the spanwise periodic streaks in the naphthalene and for the secondary instability leading to transition.[16]

Four different chord locations and three different heights in the boundary layer are chosen for hot-wire scans. These sensitive (and tedious) measurements require very long run times. The Arizona State University Unsteady Wind Tunnel does not have an active cooling system, and so hot-wire temperature drift could be a potential problem. However, this is obviated by applying a software temperature-compensation technique[22] during the test runs and also during calibration of the wires.

Figure 9 shows the results at $x/c = 0.35$ and also shows a modulation in the streamwise velocity over the entire scan and a strong modulation in the region influenced by the roughness element. Tracing the streamline downstream from the roughness element would locate it at $z = 25$ mm in Fig. 9. The disturbances take the form of a wave packet that is confined to a region of roughly $z = 0$–50 mm in the scan. The remaining portion of the scan shows a lower level modulation caused by the background crossflow level along with any noise in the measurement process. The strongest gradients in u' occur well up in the boundary layer, as documented by Kohama et al.[16]

The streamwise growth of the vortices can be seen in Fig. 10, which shows a three-dimensional representation of the hot-wire data taken at $\bar{u}/U_e = 0.5$. The scans have been aligned so that the streamline of the roughness element is centered at $z = 25$ mm. At $x/c = 0.25$, the streamwise velocity distortions are already sizable and the enhanced vortices behind the roughness can already be seen near $z = 25$ mm. The distortions grow dramatically back to $x/c = 0.40$, which is near the start of the transition wedge. One also sees a spreading of the wave packet as it grows and travels downstream. This is due to a slight difference in the propagation direction of the spectral components of the wave packet.[23]

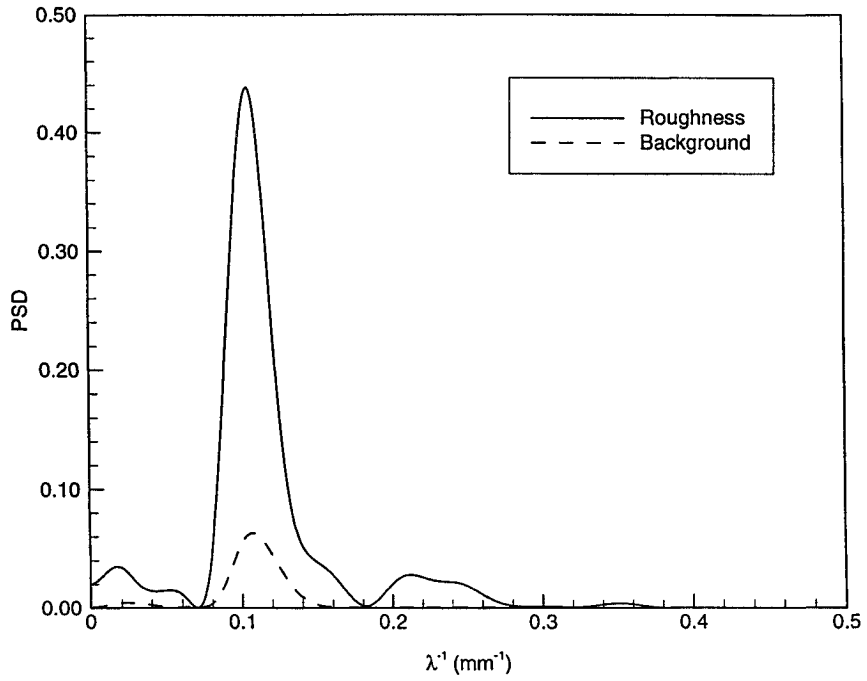

Fig. 11 Spatial power spectrum of streamwise velocity from spanwise hot-wire scan; mean velocity $\bar{u}/U_e$ subtracted; hanning window used; power spectral density is normalized to preserve mean-squared power of spatial data after integration.

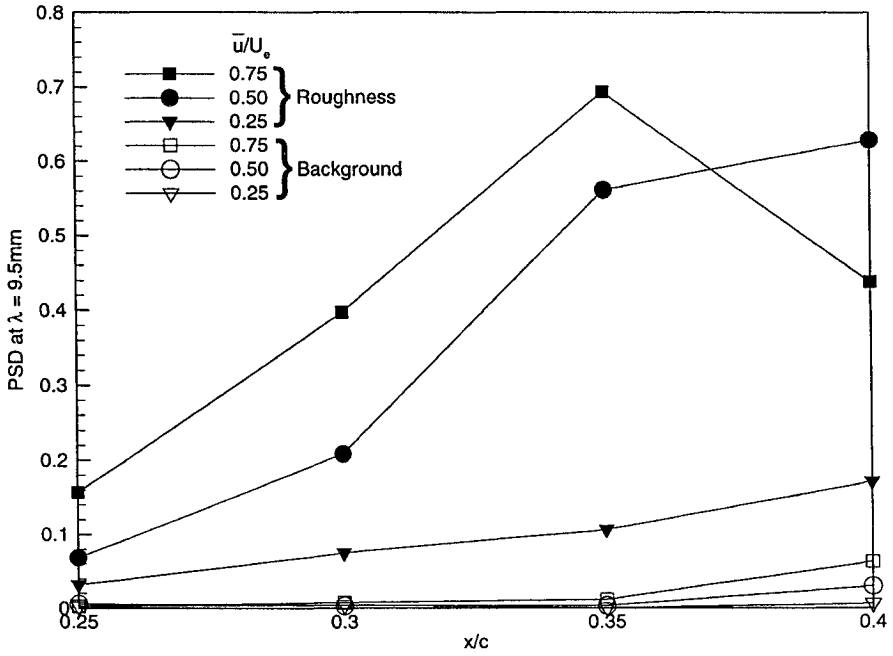

Fig. 12 Growth of dominant ($\lambda_{cf} = 8$ mm) crossflow mode with and without roughness; $Re_c = 2.6 \times 10^6$; single roughness element with $D = 3.7$ mm, $k = 6$ μm is at $x/c = 0.023$.

A spectral analysis, as seen in Fig. 11, gives a view of the wavelength content of the crossflow pattern and provides a means for quantitatively measuring the impact of the roughness on the crossflow waves. In Fig. 11, the curve labeled "Roughness" shows a spatial power spectrum of the first half of the spanwise hot-wire scan at $x/c = 0.4$ and $\bar{u}/U_e = 0.75$. This portion of the scan contains the roughness-induced wave packet, as observed in Figs. 9 and 10. The curve labeled "Background" is a spatial power spectrum from the second half of the same scan and shows the modal content of the crossflow in the region not influenced by the roughness. In both cases, the dominant crossflow component at $x/c = 0.4$ is a band centered around $\lambda = 9.5$ mm, which gives $\lambda_{cf} = 8$ mm when projected in the direction of the crossflow wave vector. This spectrum is measured near the beginning of the transition wedge and is a result of a complicated selection process involving the initial roughness spectrum, the receptivity process, and both linear and nonlinear propagation of the stationary crossflow modes. Figure 11 dramatically shows the influence of the roughness on the dominant crossflow modes. The spectrum also shows some background content that is a combination of other parts of the wave packet spectrum, leakage from the main spectral peak due to the limited sample size, background crossflow components, and instrumentation errors. Among the many choices available, one method of measuring quantitatively the crossflow amplitude and the effect of the roughness is to measure the amplitude of the power spectral density at the most amplified wavelength. This method is chosen here because it removes some of the complexity in the results due to the additional components in the spectrum.

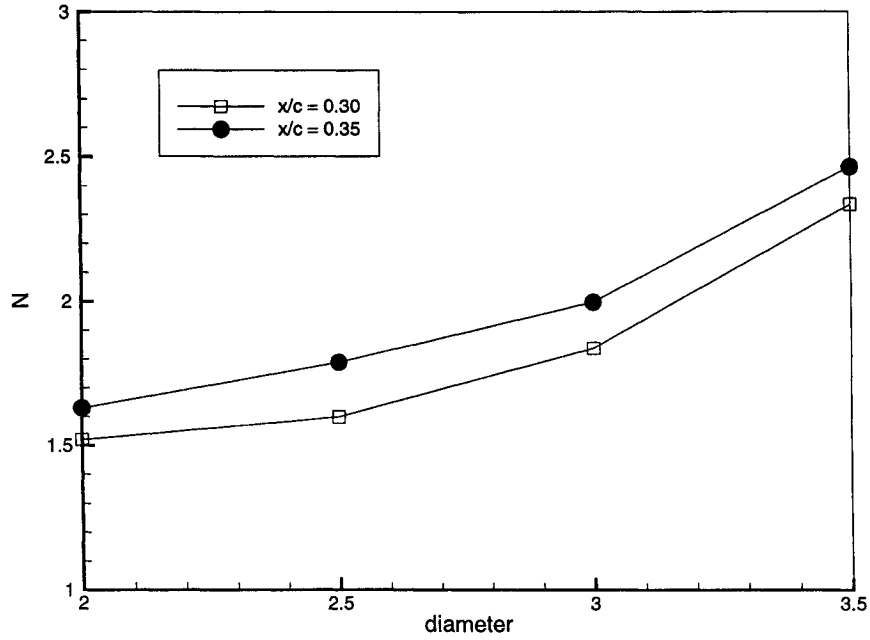

Fig. 13 Magnitude of dominant ($\lambda_{cf} = 8$ mm) crossflow mode with varying roughness diameter; $Re_c = 2.6 \times 10^6$; single roughness element with $k = 6$ μm is at $x/c = 0.023$.

Figure 12 shows a result of the discribed spectral amplitude measurement at $\lambda_{cf} = 8$ mm for the four chord positions and three mean boundary-layer positions measured in the test. The data at all positions clearly show the impact of the roughness on the system by providing higher initial amplitudes for the dominant crossflow modes, which leads to high amplitudes at earlier x/c than for the background case. At $x/c = 0.4$ (just before transition), the nonlinear saturation has caused a change in the profile of the dominant mode. Note that in the background scans, the amplitudes of the dominant mode are far below the transitional amplitudes of the roughness-produced wave packet, which is consistent with the much higher x_{tr}/c without the roughness.

The degree of crossflow enhancement increases dramatically with the roughness diameter as indicated in Fig. 13. This is consistent with the variation of transition location with roughness size and emphasizes the point that crossflow transition N factors are tied directly to the initial conditions provided by the surface-roughness spectrum at the attachment line.

III. Conclusions

A. Specific Conclusions from Present Results

We have shown that micrometer-sized roughness can strongly influence crossflow-dominated transition, and the effect of roughness height and roughness diameter is quantified for the circular roughness shapes tested here. This effect is confined to roughness near the attachment line and is tied directly to the coupling of the initial roughness spectrum with the dominant crossflow modes through the receptivity process. The stationary crossflow modes do not appear to be influenced by acoustic disturbances, in contrast with T–S waves.

B. General Conclusions on Crossflow-Dominated Transition

The $\alpha = -4$ deg condition of the present experiment is completely subcritical to T–S wave growth. The growth is stretched to 71% chord (the pressure minimum) so that the boundary-layer thickness is large (3 mm). On an actual flight airfoil, the pressure minimum would, of course, be forward of this. However, the basic idea has always been that the effects of both Reynolds number and fetch are included in the N factor. Thus, we can compare transition at 40% chord in these experiments with, for example, 15% chord in flight because the N factors would be the same. Therefore, the final interpretation of our data should be in terms of the change in N and not in the change in location. The utility of these experiments is that we can measure sensitive phenomena in a quantitative way and be able to see the difference between 0.25- and 0.5-μm roughness. At the same time, of course, we can see that the 6-μm roughness changes N by 3.

We have shown before that, when transition is crossflow dominated in a low-disturbance environment, the stationary crossflow wave is the dominant instability that causes transition even though theory may predict that traveling crossflow waves are more amplified.[16] The role of three-dimensional roughness is to provide a source of streamwise vorticity that influences the initial amplitude of the stationary wave. We have found that the low-amplitude roughness (6 μm) influences transition until the roughness diameter is a small fraction of the crossflow wavelength (see Figs. 7 and 8). This is consistent with our conjecture that the relation of the roughness parameters (and the resulting spectrum of the roughness) to the wavelengths of the dominant stationary crossflow modes is of primary importance in determining the transition behavior. If the roughness diameter exceeds $0.08\lambda_{cf}$, we can see the change in transition location regardless of roughness height. An increase in height decreases N.

We can conclude the following. In a low-disturbance environment, stationary crossflow vortices dominate transition via a high-frequency secondary instability.[16] The initial conditions (receptivity) are determined by surface roughness; hence, roughness influences transition N factors. Isolated roughness influences transition until the diameter is much less than the crossflow wavelength. Roughness Reynolds numbers Re_k in the range of 1–4 can change N by 3. Distributed roughness (random) appears to have the dangerous scales that effect transition. In a high-turbulence environment, traveling crossflow waves dominate transition,[12,13] and the saw-toothed pattern of transition is not strong. One may conjecture that roughness is not as important in this case.

Acknowledgments

The experimental work was supported by NASA Langley Research Center Grant NAG1-937. R. H. Radeztsky was supported by NASA Langley Research Center Fellowship NAG1-1111, and M. S. Reibert was supported by the Office of Naval Research Fellowship Program. The authors would like to thank Shohei Takagi for his contributions to the preliminary phase of this work. The invaluable help of D. Clevenger, who polished the model and prepared the roughness samples, and D. J. Orr, who measured and analyzed the roughness samples, is gratefully acknowledged. Thomas Corke suggested the use of dental acrylics.

References

[1]Reed, H. L., and Saric, W. S., "Stability of Three-Dimensional Boundary Layers," *Annual Review of Fluid Mechanics*, Vol. 21, 1989, pp. 235–284.

[2]Reed, H. L., Saric, W. S., and Arnal, D., "Linear Stability Theory Applied to Boundary Layers," *Annual Review of Fluid Mechanics*, Vol. 28, 1996, pp. 389–428.

[3]Somers, D. M., and Horstmann, K. H., "Design of a Medium-Speed Natural-Laminar-Flow Airfoil for Commuter Aircraft Applications," DFVLR, Rept. IB/29-85/26, Göttingen, Germany, July 1985.

[4]Dagenhart, J. R., "Crossflow Disturbance Measurements on a 45 Degree Swept Wing," Ph.D. Dissertation, Dept. of Engineering Mechanics, Virginia Polytechnic Inst. and State Univ., Blacksburg, VA, Dec. 1992.

[5]Kaups, K., and Cebeci, T., "Compressible Laminar Boundary Layers with Suction on Swept and Tapered Wings," *Journal of Aircraft*, Vol. 14, No. 7, 1977, pp. 661–667.

[6]Reibert, M. S., "Nonlinear Stability, Saturation, and Transition in Crossflow-Dominated Boundary Layers," Ph.D. Dissertation, Dept. of Mechanical and Aerospace Engineering, Arizona State Univ., Tempe, AZ, May 1996.

[7]Dagenhart, J. R., "Amplified Crossflow Disturbances in the Laminar Boundary Layer on Swept Wings with Suction," NASA TP-1902, 1981.

[8]Saric, W. S., Dagenhart, J. R., and Mousseux, M. C., "Experiments in Swept-Wing Transition," *Numerical and Physical Aspects of Aerodynamic Flows*, Vol. 4, edited by T. Cebeci, Springer–Verlag, Berlin, 1990, pp. 359–415.

[9]Dagenhart, J. R., Saric, W. S., Mousseux, M. C., and Stack, J. P., "Crossflow-Vortex Instability and Transition on a 45-Degree Swept Wing," AIAA Paper 89-1892, June 1989.

[10]Dagenhart, J. R., Saric, W. S., Hoos, J. A., and Mousseux, M. C., "Experiments on Swept-Wing Boundary Layers," *Laminar-Turbulent Transition*, Vol. 3, edited by D. Arnal, Springer–Verlag, Berlin, 1990, pp. 369–380.

[11]Saric, W. S., Reed, H. L., and Kerschen, E. J., "Leading-Edge Receptivity to Sound," AIAA Paper 94-2222, June 1994.

[12]Bippes, H., and Müller, B., "Disturbance Growth in an Unstable Three-Dimensional Boundary Layer," *Numerical and Physical Aspects of Aerodynamic Flows*, Vol. 4, edited by T. Cebeci, Springer–Verlag, Berlin, 1990, pp. 345–358.

[13]Bippes, H., "Experiments on Transition in Three-Dimensional Accelerated Boundary Layer Flows," *Proceedings of the Royal Aeronautical Society: Boundary Layer Transition and Control*, edited by M. Gaster, Royal Aeronautical Society, Cambridge, England, UK, 1991.

[14]Deyhle, H., Höhler, G., and Bippes, H., "Experimental Investigation of Instability Wave Propagation in a Three-Dimensional Boundary-Layer Flow," *AIAA Journal*, Vol. 31, No. 4, 1993, pp. 637–645.

[15]Deyhle, H., and Bippes, H., "Disturbance Growth in an Unstable Three-Dimensional Boundary Layer and Its Dependence on Environmental Conditions," *Journal of Fluid Mechanics*, Vol. 316, 1996, pp. 73–113.

[16]Kohama, Y., Saric, W. S., and Hoos, J. A., "A High-Frequency Secondary Instability of Crossflow Vortices that Leads to Transition," *Proceedings of the Royal Aeronautical Society: Boundary Layer Transition and Control*, edited by M. Gaster, Royal Aeronautical Society, Cambridge, England, UK, 1991.

[17]Mangalam, S. M., Maddalon, D. V., Saric, W. S., and Agarwal, N. K., "Measurements of Crossflow Vortices, Attachment-Line Flow, and Transition Using Microthin Hot Films," AIAA Paper 90-1636, June 1990.

[18]von Doenhoff, A. E., and Braslow, A. L., "The Effect of Distributed Surface Roughness on Laminar Flow," *Boundary Layer Control*, Vol. 2, edited by V. Lachmann, Pergamon, Oxford, 1961, pp. 657–681.

[19]Juillen, J. C., and Arnal, D., "Etude Expérimentale du dé Clenchement de la Transition par Rugosités et par Rainer sur de Bord d'Attaque d'une Aile en Flèche en Ènçoulement Incompressible," CERT/ONERA, Rapport Final No. 51/5018.35, Toulouse, France, June 1990.

[20]Choudhari, M., "Roughness-Induced Generation of Crossflow Vortices in Three-Dimensional Boundary Layers," *Theoretical and Computational Fluid Dynamics*, Vol. 6, 1994, pp. 1–30.

[21]Saric, W. S., Hoos, J. A., and Radeztsky, R. H., "Boundary-Layer Receptivity of Sound with Roughness," *Boundary Layer Stability and Transition to Turbulence*, edited by D. C. Reda, H. L. Reed, and R. Kobayashi, FED Vol. 114, American Society of Mechanical Engineers, New York, 1991, pp. 17–22.

[22]Radeztsky, R. H., Jr., Reibert, M. S., and Takagi, S., "A Software Solution to Temperature-Induced Hot-Wire Voltage Drift," *Proceedings of the Third International Symposium on Thermal Anemometry*, FED Vol. 167, American Society of Mechanical Engineers, Washington, DC, 1993, pp. 49–55.

[23]Mack, L. M., "The Wave Pattern Produced by a Point Source on a Rotating Disk," AIAA Paper 85-0490, Jan. 1985.

R. Wlezien
Associate Editor